5 Supersonic flow over a thin airfoil at zero lift: D'Alembert solution

In this chapter we will find an analytical solution for the supersonic ($M_\infty > 1$) potential flow around a thin symmetric airfoil aligned with a horizontal incoming flow, as sketched in Figure 3. The profile of small thickness $\epsilon \ll 1$ causes a small perturbation of the outer potential flow. The small perturbation is described by Eq. (4.22) with the boundary conditions (4.24), (4.26), (4.30) and (4.32). For $M_\infty > 1$, Eq. (4.22) is a wave equation. Thus, it can be solved with the D'Alembert solution, as described, e.g., by Lebl (2025). In this chapter we will show how the D'Alembert solution can be used to satisfy the boundary conditions of the present problem.

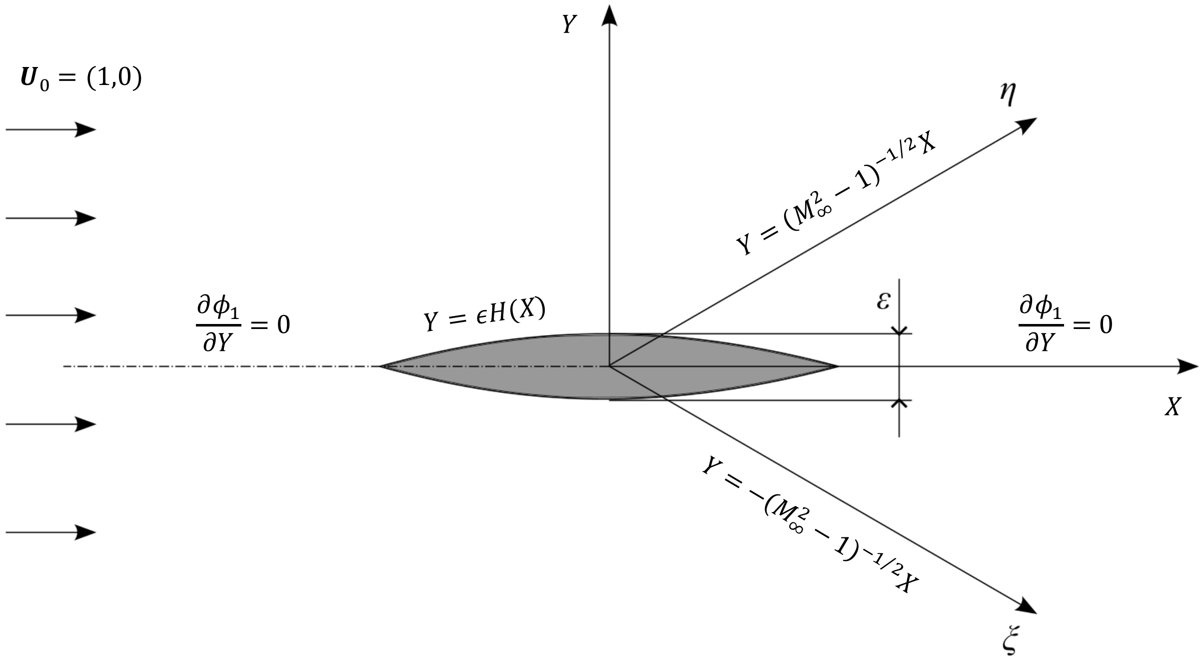

Figure 4: Sketch of the dimensionless problem formulation and the new coordinate axes.

5.1 Change of variables

We transform the problem into a new coordinate system aligned with the characteristics

$$\xi = X - \sqrt{M_\infty^2 - 1}\, Y,\ \eta = X + \sqrt{M_\infty^2 - 1}\, Y \tag{5.1}$$

and search for a solution $\tilde{\phi}$ in the new coordinate system such that

$$\phi_1(X, Y) = \tilde{\phi}\big(\xi(X, Y), \eta(X, Y)\big). \tag{5.2}$$

The coordinate axes are sketched in Figure 4. The transformed wave equation (4.22) in the new coordinate system reads

$$\frac{\partial^2 \tilde{\phi}}{\partial \xi \partial \eta} = 0. \tag{5.3}$$

The solution of the transformed wave equation takes the following form:

$$\tilde{\phi} = f(\xi) + g(\eta), \tag{5.4}$$

which can be transformed back to the original coordinate system as

$$\phi_1 = f\left(X - \sqrt{M_\infty^2 - 1}\,Y\right) + g\left(X + \sqrt{M_\infty^2 - 1}\,Y\right). \tag{5.5}$$

The functions *f* and *g* are determined by the boundary conditions.

5.2 Boundary conditions

Since boundary conditions are prescribed along the symmetry plane $Y = 0$, we must split the domain into an upper side ($Y > 0$) and a lower side ($Y < 0$). The solutions in the upper and the lower side are reflection symmetric about $Y = 0$.

Incoming flow condition

First, we employ the far-field condition (4.24), which in the new coordinate system transforms to

$$\tilde{\phi} \to 0 \quad \text{as} \quad \begin{cases} \xi \to -\infty, & \text{for } Y > 0 \\ \eta \to -\infty, & \text{for } Y < 0 \end{cases}. \tag{5.6}$$

Therefore,

$$\begin{cases} g(\eta) = \text{const.} = -f(-\infty) & \text{for } Y > 0\,, \\ f(\xi) = \text{const.} = -g(-\infty) & \text{for } Y < 0\,. \end{cases} \tag{5.7}$$

We can conveniently set the constants to 0 such that

$$\tilde{\phi} = \begin{cases} f(\xi) & \text{for } Y > 0 \\ g(\eta) & \text{for } Y < 0 \end{cases} \tag{5.8}$$

and

$$\begin{aligned} f &\to 0 \quad \text{as} \quad \xi \to -\infty, \\ g &\to 0 \quad \text{as} \quad \eta \to -\infty. \end{aligned} \tag{5.9}$$

Symmetry condition

Next, we transform the symmetry condition (4.26) to the new variables. Using the Ansatz (5.8), the left-hand side of Eq. (4.26) can be expressed with the chain rule as follows:

$$\frac{\partial \phi_1}{\partial Y} = \begin{cases} \dfrac{\partial \xi}{\partial Y}\dfrac{\mathrm{d}f}{\mathrm{d}\xi} = -\sqrt{M_\infty^2 - 1}\,f' & \text{for } Y > 0 \\ \dfrac{\partial \eta}{\partial Y}\dfrac{\mathrm{d}g}{\mathrm{d}\eta} = \sqrt{M_\infty^2 - 1}\,g' & \text{for } Y < 0 \end{cases}. \tag{5.10}$$

With the transformation (5.1) we can determine the positions of the leading and the trailing edges in the new coordinate system as

$$\begin{aligned} (X, Y) &= (-1/2\,, 0) \implies (\xi, \eta) = (-1/2\,, -1/2), \\ (X, Y) &= (\ \ 1/2\,, 0) \implies (\xi, \eta) = (\ \ 1/2, \ \ 1/2), \end{aligned} \tag{5.11}$$

respectively. Thus, the transformed symmetry condition (4.26) reads

$$\begin{aligned} f' &= 0 \quad \text{for } \xi < -1/2 \ \vee \ \xi > 1/2\,, \\ g' &= 0 \quad \text{for } \eta < -1/2 \ \vee \ \eta > 1/2\,. \end{aligned} \tag{5.12}$$

Integrating the symmetry condition (5.12) we obtain

$$f(\xi < -1/2) = a, \qquad f(\xi > 1/2) = b, \qquad g(\eta < -1/2) = c, \qquad g(\eta > 1/2) = d\,. \tag{5.13}$$

From the far-field condition (5.9) we can determine

$$a = c = 0. \tag{5.14}$$

Furthermore, the velocity potential must be continuous at the symmetry plane $Y = 0$ behind the airfoil ($X > 1/2$). Thus,

$$b = d. \tag{5.15}$$

Kinematic condition

Finally, we transform the flow-tangency condition at the airfoil, Eqs. (4.30) and (4.32), using Eq. (5.10) to obtain

$$\begin{aligned} -\sqrt{M_\infty^2 - 1}\, f'(\xi) &= \;\; H'(\xi) \quad \text{for } -1/2 < \xi < 1/2, \\ \sqrt{M_\infty^2 - 1}\, g'(\eta) &= -H'(\eta) \quad \text{for } -1/2 < \eta < 1/2. \end{aligned} \tag{5.16}$$

Integration of Eq. (5.16) leads to

$$\begin{aligned} f(\xi) &= -(M_\infty^2 - 1)^{-\frac{1}{2}} H(\xi) + j \quad \text{for } -1/2 < \xi < 1/2, \\ g(\eta) &= -(M_\infty^2 - 1)^{-\frac{1}{2}} H(\eta) + k \quad \text{for } -1/2 < \eta < 1/2. \end{aligned} \tag{5.17}$$

Again, we must ensure a continuous velocity potential at the boundaries between different intervals by matching the integration constants. With sufficient generality we can assume that the normalized thickness function H of the profile is zero at the leading and the trailing edges, that is, $H(-1/2) = H(1/2) = 0$. Requiring the velocity potential $\tilde{\phi}$ defined by Eqs. (5.13), (5.14) and (5.17) to be continuous across the characteristics $\xi = -1/2$ and $\eta = -1/2$ passing through the leading edge we have, respectively,

$$\begin{aligned} f(-1/2) &= j = a = 0, \\ g(-1/2) &= k = c = 0. \end{aligned} \tag{5.18}$$

Analogously, at $\xi = 1/2$ and $\eta = 1/2$ we match the constants

$$b = d = 0. \tag{5.19}$$

5.3 Result: Analytical velocity potential as a piecewise function

The expression for the analytical velocity potential reads

$$\tilde{\phi} = \begin{cases} -(M_\infty^2 - 1)^{-\frac{1}{2}} H(\xi), & Y > 0 \wedge -1/2 < \xi < 1/2 \\ -(M_\infty^2 - 1)^{-\frac{1}{2}} H(\eta), & Y < 0 \wedge -1/2 < \eta < 1/2 \\ 0, & \text{otherwise} \end{cases}. \tag{5.20}$$

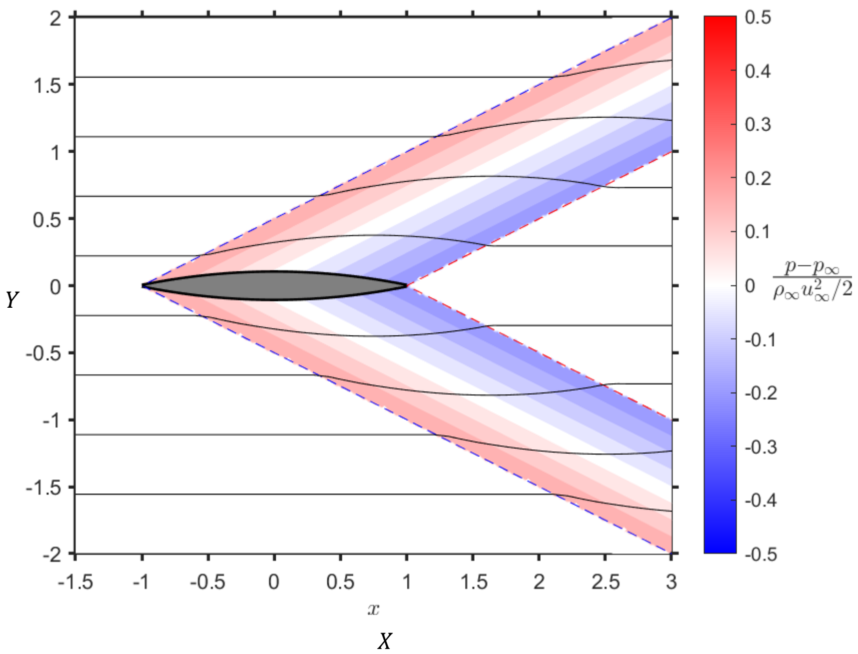

Figure 5: Example of the analytical solution for a given profile shape. Color shows the pressure field and black solid lines are the streamlines of the flow. Dashed lines show the characteristics originating from the leading and trailing edges.

5.4 Exercise

Plot the velocity vectors of the supersonic flow at $M_\infty = 2$ over a slender airfoil with the shape defined by

$$H(X) = 1/2 - 2X^2 \quad \text{for} -1/2 < X < 1/2 \tag{5.21}$$

and $\epsilon = 0.1$.

5.5 Literature

- For more details about the D'Alembert solutions of the wave equation, see Lebl (2025).

References

Bigarella, E. D. V., Chilvers, J., Demirel, E., & Romanó, F. (2015). *CFD Education Center*. https://cfdblogvienna.blogspot.com/

Brennen, C. E. (2004). *Internet Book on Fluid Dynamics*. Caltech. http://brennen.caltech.edu/FLUIDBOOK/front1.htm

Chattot, J.-J. (2002). Partial Differential Equations. In *Computational Aerodynamics and Fluid Dynamics*. Springer-Verlag Berlin.

Fletcher, C. (1998). Partial Differential Equations. In *Computational Techniques for Fluid Dynamics 1: Fundamental and General Techniques*. Springer.

Hosseini, M., Vinuesa, R., Hanifi, A., Henningson, D., & Schlatter, P. (2015, November 22). Video: Turbulent flow around a wing profile, a direct numerical simulation. *68th Annual Meeting of the APS Division of Fluid Dynamics - Gallery of Fluid Motion*. https://doi.org/10.1103/APS.DFD.2015.GFM.V0078

Hosseini, S. M., Vinuesa, R., Schlatter, P., Hanifi, A., & Henningson, D. S. (2016). Direct numerical simulation of the flow around a wing section at moderate Reynolds number. *International Journal of Heat and Fluid Flow*, *61*, 117–128. https://doi.org/10.1016/j.ijheatfluidflow.2016.02.001

Kuhlmann, H. C. (2021). Klassifizierung partieller Differentialgleichungen. In *Numerische Methoden der Strömungs- und Wärmetechnik*. TU Wien [lecture notes for the course No. 302.017]. https://www.fluid.tuwien.ac.at/HendrikKuhlmann?action=AttachFile&do=get&target=Numerik_I.web.pdf

Lebl, J. (2025). D'Alembert Solution of The Wave Equation. In *Differential Equations for Engineers* (pp. 4.8.1-4.8.4). Oklahoma State University. https://math.libretexts.org/@go/page/342?pdf

Moran, J. (1984). *An Introduction to Theoretical and Computational Aerodynamics*. Wiley.

Otto, A. (2011). Classification of PDEs and Related Properties. In *Methods of Numerical Simulation in Fluids and Plasmas*. University of Alaska [lecture notes]. http://www.mediafire.com/view/qzqfu2cznq556y0/Classification_of_PDEs.pdf

Prandtl, L., Oswatitsch, K., & Wieghardt, K. (1993). *Führer durch die Strömungslehre* (9th ed.). Vieweg.

Schneider, W. (1978). *Mathematische Methoden der Strömungsmechanik*. Vieweg. https://doi.org/10.1007/978-3-322-83943-5

Steinrück, H. (2020). *Asymptotische Methoden der Strömungsmechanik*. TU Wien [lecture notes for the course No. 322.074].

Van Dyke, M. (1982). *An Album of Fluid Motion*. The Parabolic Press.

Wesseling, P. (2001). Classification of partial differential equations. In *Principles of Computational Fluid Dynamics* (1st ed.). Springer. https://doi.org/10.1007/978-3-642-05146-3